

Low field hysteresis in disordered ferromagnets

Lorenzo Dante¹, Gianfranco Durin², Alessandro Magni² and Stefano Zapperi¹

¹ *INFM unità di Roma 1, Dipartimento di Fisica, Università "La Sapienza", P.le A. Moro 2 00185 Roma, Italy*

² *Istituto Elettrotecnico Nazionale Galileo Ferraris and INFM, Corso M. d'Azeglio 42, I-10125 Torino, Italy*

We analyze low field hysteresis close to the demagnetized state in disordered ferromagnets using the zero temperature random-field Ising model. We solve the demagnetization process exactly in one dimension and derive the Rayleigh law of hysteresis. The initial susceptibility a and the hysteretic coefficient b display a peak as a function of the disorder width. This behavior is confirmed by numerical simulations $d = 2, 3$ showing that in limit of weak disorder demagnetization is not possible and the Rayleigh law is not defined. These results are in agreement with experimental observations on nanocrystalline magnetic materials.

PACS numbers: 75.60.Ej, 75.60.Ch, 64.60.Ht, 68.35.Ct

Ferromagnetic materials display hysteresis under the action of an external field and the magnetization depends in a complex way on the field history. In order to define magnetic properties unambiguously, it is customary to first *demagnetize* the material, bringing it to a state of zero magnetization at zero field. This can be done, in practice, by the application of a slowly varying AC field with decreasing amplitude. In this way, the system explores a complex energy landscape, due to the interplay between structural disorder and interactions, until it is trapped into a low energy minimum. This demagnetized state is then used as a reference frame to characterize the magnetic properties of the material.

The hysteresis properties at low fields, starting from the demagnetized state, have been investigated already in 1887 by Lord Rayleigh [1], who found that the branches of the hysteresis loop are well described by parabolas. In particular, when the field is cycled between $\pm H^*$, the magnetization M follows $M = (a + bH^*)H \pm b((H^*)^2 - H^2)/2$, where the signs \pm distinguish the upper and lower branch of the loop. Consequently the area of the loop scales with the peak field H^* as $W = 4/3b(H^*)^3$ and the response to a small field change, starting from the demagnetized state is given by $M^* = a(H^*) \pm b(H^*)^2$ [2].

The Rayleigh law has been widely observed in ferromagnetic materials [2], but also in ferroelectric ceramics [3,4] and in type II superconductors [5]. The current theoretical interpretation of this law is based on a 1942 paper by Néel [6], who derived the law formulating the magnetization process as the dynamics of a point (i.e. the position of a domain wall) in a random potential. In this framework, the initial susceptibility a is associated to reversible motions inside one of the many minima of the random potential, while the hysteretic coefficient b is due to irreversible jumps between different valleys. Successive developments and improvements have been devoted to establish precise links between Néel random potential and the material microstructure [7–10], but in several cases the issue is still unsettled. For instance, the initial permeability of nanocrystalline materials typically displays a peak as a function of the grain size [11],

heat treatment [12,13] or alloy composition [11,14]. This behavior can be associated to changes in the disordered microstructure, but can not be accounted for by Néel theory that predicts a monotonic dependence of a from the disorder width [6].

The zero temperature random-field Ising model (RFIM) has been recently used to describe the competition between quenched disorder and exchange interactions and their effect on the hysteresis loop [15]. In three and higher dimensions, the model shows a phase transition between a continuous cycle for strong disorder and a discontinuous loop, with a macroscopic jump, at low disorder. The two phases are separated by a second order critical point, characterized by universal scaling laws [15–17]. A behavior of this kind is not restricted to the RFIM but has also been observed in other models, with random bonds [18], random anisotropies [19] or vectorial spins [20]. In addition, a similar disorder induced phase transition in the hysteresis loop has been experimentally reported for a Co-Co0 bilayer [21]. Thus the RFIM provides a tractable model for a more generic behavior: the model has been solved exactly in one dimension [22,23] and on the Bethe lattice [24–26], while mean-field theory [15] and renormalization group [16] have been used to analyze the transition.

Here, we use the RFIM to analyze the demagnetization process and investigate the properties of the hysteresis loop at low fields. Along the lines of Refs. [23,26], we compute the demagnetization cycles exactly in one dimension and derive the Rayleigh law, obtaining a and b as function of disorder and exchange energies. Next, we analyze the problem numerically in higher dimensions (i.e. $d = 2$ and $d = 3$) where exact results are at present not available. In $d = 3$, we find that the disorder induced transition [15], defined on the saturation loop, is also reflected by the Rayleigh loops: in the weak disorder phase the system can not be demagnetized, as the final magnetization coincides with the saturation magnetization. A similar behavior has been recently obtained analyzing subloops [27]. In the high disorder phase, however, a demagnetization process is possible and hysteresis loops are still described by the Rayleigh law, with parameters

scaling to zero at the transition. Above the transition, the dependence of a and b on disorder is qualitatively similar in all dimensions, displaying a peak and decreasing to zero for very strong disorder in agreement with experiments [11–14].

In the RFIM, a spin $s_i = \pm 1$ is assigned to each site i of a d -dimensional lattice. The spins are coupled to their nearest-neighbors spins by a ferromagnetic interaction of strength J and to the external field H . In addition, to each site of the lattice it is associated a random field h_i taken from a Gaussian probability distribution with variance R , $\rho(h) = \exp(-h^2/2R^2)/\sqrt{2\pi R}$. The Hamiltonian thus reads

$$E = - \sum_{\langle i,j \rangle} J s_i s_j - \sum_i (H + h_i) s_i, \quad (1)$$

where the first sum is restricted to nearest-neighbors pairs. The dynamics proposed in Ref. [28] and used in Refs. [15–17] is such that the spins align with the local field

$$s_i = \text{sign}(J \sum_j s_j + h_i + H). \quad (2)$$

In this way a single spin flip can lead the neighboring spins to flip, eventually triggering an avalanche.

It has been shown that the RFIM obeys return-point memory [15]: if the field is increased adiabatically the magnetization only depends on the state in which the field was last reversed. This property has been exploited in $d = 1$ to obtain exactly the saturation cycle and the first minor loops [23]. Similar results have been also reported for the Bethe lattice [26]. Here, we extend this approach to more general field histories, treating explicitly the demagnetization process: the external field is changed through a nested succession $H = H_0 \rightarrow -H_1 \rightarrow H_2 \rightarrow \dots (-1)^n H_n \dots \rightarrow 0$, with $H_{n-1} > H_n > H_{n+1} > 0$ and $dH \equiv H_n - H_{n-1} \rightarrow 0$. The initial value H_0 should correspond to complete saturation, but one can show that as long as $H_n \geq J$ the magnetization M_n just follows the saturation curve. Thus we can safely set $H_0 = J$.

As in Ref. [23], the key quantity to compute is the conditional probability U_{2n} that a spin flips up before its nearest neighbor when the field is increased from $-H_{2n-1}$ to H_{2n} . Similarly on descending loops we define D_{2n+1} as the conditional probability that a spin flips down before its nearest neighbor when the field is decreased from H_{2n} to $-H_{2n+1}$. Enumerating all possible spin histories, we find recursion relations for the conditional probabilities which read as [29]

$$U_{2n} = U_{2n-2} + \left[\frac{U_{2n-2}(p_1(H_{2n}) - p_1(H_{2n-2})) + D_{2n-1}(p_0(H_{2n}) - p_0(H_{2n-2}))}{1 - (p_1(H_{2n}) - p_1(-H_{2n-1}))} \right], \quad (3)$$

$$D_{2n+1} = D_{2n-1} + \left[\frac{D_{2n-1}(p_1(-H_{2n-1}) - p_1(-H_{2n+1})) + U_{2n}(p_2(-H_{2n-1}) - p_2(-H_{2n+1}))}{1 - (p_1(H_{2n}) - p_1(-H_{2n+1}))} \right], \quad (4)$$

where $p_k(H) = \int_{2(1-k)J-H}^{\infty} \rho(x) dx$ is the probability for a spin to be up when k nearest-neighbors are up. The magnetization as a function of the peak field is given by

$$\begin{aligned} M_{2n} &= M_{2n-1} + 2U_{2n}^2(p_2(H_{2n}) - p_2(-H_{2n-1})) \\ &+ 4U_{2n}D_{2n-1}(p_1(H_{2n}) - p_1(-H_{2n-1})) + \\ &2D_{2n-1}^2(p_0(H_{2n}) - p_0(-H_{2n-1})) \end{aligned} \quad (5)$$

and a similar expression holds for M_{2n+1} . In the limit $dH \rightarrow 0$, $H_n \rightarrow H^*$, Eqs. 3-4 relations become a pair of differential equations, but exploiting the symmetry $U(H^*) = D(-H^*)$, we can reduce the problem to a single equation

$$\frac{dU}{dH^*} = U \frac{\rho(H^*) + \rho(2J - H^*)}{1 - \Delta(H^*)}, \quad (6)$$

with $\Delta = \int_{-H^*}^{H^*} \rho(x) dx$ and the boundary conditions is the conditional probability computed on the saturation

loop $U(J) = 1/2$. Eq. 6 can be easily solved, and the result reads

$$U = \frac{1}{2} \exp \left[- \int_{H^*}^J \frac{\rho(x) + \rho(2J - x)}{1 - \Delta(x)} dx \right]. \quad (7)$$

Once the conditional probability U is known, it is straightforward to compute the magnetization as a function of the peak field H^* from Eq. 5, noting that $M(-H^*) = -M(H^*)$. Inner loops starting from the demagnetization curve (i.e. Eq. 5) can also be computed exactly. In Fig. 1 we report an example of the saturation loop, together with demagnetization curve and a few inner loops. The analytical results are compared with numerical simulations, performed on a lattice with $L = 5 \cdot 10^5$ spins, using a single realization of the disorder. The perfect agreement between the curves confirms that the magnetization is self-averaging, as assumed throughout the calculations.

Expanding the demagnetization curve around $H^* = 0$, we obtain $M \simeq aH^* + b(H^*)^2$ recovering the Rayleigh expression with $a = 4U(0)^2(\rho(0) + \rho(2J))$ and $b =$

$8U(0)^2(\rho(0) + \rho(2J))^2$. An expansion can also be performed for minor loops on the demagnetization curve (i.e. cycling H between $\pm H^*$), yielding $M = (a + bH^*)H \pm b((H^*)^2 - H^2)/2$, which coincides with the Rayleigh law. In Fig. 2 we report the values of a and b as a function of the disorder R , showing that both components of the susceptibility display a maximum in R . To identify the low and strong disorder behavior of the susceptibilities, we perform an asymptotic expansion and obtain that $a \sim \exp[-(J^2/(2R^2))]$ for $R \rightarrow 0$ and $a \sim 1/R$ for $R \rightarrow \infty$. The parameter b follows similar laws.

Next, we turn our attention to higher dimensional system, for which analytical results are not available. In order to obtain unambiguously the demagnetized state for a given realization of the disorder, one should perform a *perfect demagnetization*. This is done in practice changing the field by precisely the amount necessary to flip the first unstable spin [17]. In this way, the field is cycled between $-H^*$ and H^* and H^* is then decreased at the next cycle by precisely the amount necessary to have one avalanche less than in the previous cycle. This corresponds to decrease H^* at each cycle by an amount dH , with $dH \rightarrow 0^+$. The perfect demagnetization algorithm allows to obtain a precise characterization of the demagnetized state but it is computationally very demanding. Thus we resort to a different algorithm which perform an *approximate demagnetization*: instead of cycling the field between $-H^*$ and H^* we just flip the field between these two values and then decrease H^* by a fixed amount dH . We have checked that with a reasonably small dH (i.e. $dH < 10^{-3}$) the demagnetization curve is quite insensitive to the algorithm used.

In Fig. 2 we report the values of a and b obtained numerically in $d = 2$ and $d = 3$ for different values of R , using systems of sizes $(L = 100)^2$ and $(L = 50)^3$. The results are qualitatively similar to those obtained exactly in $d = 1$: the curve display a peak for intermediate disorder and decrease to zero for weak and strong disorder. The weak disorder limit, however, deserves a closer inspection. It is well established that in $d = 3$ the saturation loops reveal a phase transition at $R_c = 2.16$ for $J = 1$ [17] (the transition is not present in $d = 1$, while in $d = 2$ the issue is controversial [17]). We find that the transition is reflected also in the Rayleigh loops: in Fig. 3 we report the magnetization M_∞ computed using the demagnetization algorithm for different values of R . For strong disorder $R > R_c$, we see that $M_\infty \simeq 0$ as expected, but as $R < R_c$ the demagnetization curve tends to the saturation magnetization and $M_\infty \rightarrow \pm 1$. The transition becomes sharper as the system size is increased, indicating that demagnetization is possible only for $R > R_c$ (see also Ref. [27]). Next, we analyze the behavior of a and b for $R \rightarrow R_c^+$ varying the system size from $(L = 25)^3$ to $(L = 100)^3$. The results show that a and b vanish for $R \rightarrow R_c$ and follow a scaling law $a \sim b \sim (R - R_c)^{1/2}$, with very little dependence on the system size.

It is interesting to compare our theoretical results with experiments on nanocrystalline materials. It has been re-

ported that the initial susceptibility in several cases displays a peak as the heat treatment or the alloy composition are varied [11–14]. The peak is usually associated to changes in the microstructure, which induce a competition between the disorder present in grain anisotropies and inter-grain interactions mediated by the amorphous matrix [11]. Here, we see that this behavior is well captured by the RFIM, that allows to analyze the effect of the disorder-exchange ratio R/J . For weak disorder, we have a few large domains and the susceptibility is dominated by domain wall dynamics. When the disorder is increased, the number of domains (and domain walls) also increases and so does the susceptibility. Increasing the disorder further leads to a complete breakup of the domains and the response is dominated by single spin flips in low random-field regions with a progressive decrease of the susceptibility.

A detailed understanding of the demagnetization process and low field hysteresis has important implications also from a purely theoretical point of view. When a disordered system is demagnetized, it explores a complex energy landscape until it finds a metastable minimum. It would be interesting to compare the statistical properties of the demagnetized state, with those of the ground state of the system as suggested in Ref. [28]. The analysis of the ground state of disordered systems has received a wide attention in the past few years, due to the connections with general optimization problems, and the RFIM is one of the typical model used to test ground state algorithms [30]. Demagnetization could provide a relatively simple way to obtain a low energy state that can be useful for optimization procedures. We are currently pursuing investigations along these lines.

-
- [1] L. Rayleigh, Philos. Mag., Suppl. **23**, 225 (1887).
 - [2] G. Bertotti, *Hysteresis in Magnetism* (Academic Press, San Diego, 1998).
 - [3] D. Damjanovic, J. Appl. Phys. **82**, 1788 (1997). For a review see Rep. Prog. Phys. **61**, 1267 (1998).
 - [4] D. Bolten et al., Appl. Phys. Lett. **77**, 3830 (2000).
 - [5] T. Torng and Q. Y. Chen, J. Appl. Phys. **73**, 1198 (1993).
 - [6] L. Néel, Cah. Phys. **12**, 1 (1942).
 - [7] K. H. Pfeffer, Phys. Stat. Sol. **21**, 857 (1967).
 - [8] R. Vergne, Z. Blazek and J. L. Porteseil, Phys. Stat. Sol. A **25**, 171 (1974).
 - [9] H. Kronmüller and T. Reininger, J. Magn. Magn. Mat. **112**, 1 (1992).
 - [10] A. Magni, C. Beatrice, G. Durin, and G. Bertotti, J. Appl. Phys. **86**, 3253 (1999).
 - [11] G. Herzer, in *Handbook of Magnetic Materials, Vol. 10*, edited by K. H. J. Buschow (Elsevier, Amsterdam, 1997), p. 415.
 - [12] K. Suzuki, A. Makino, A. Inoue, and T. Masumoto, J.

Appl. Phys **70**, 6232 (1991).

- [13] M. S. Leu and T. S. Chin, J. Appl. Phys **81**, 4051 (1997).
 [14] S. H. Lim, W. K. Pi, T. H. Noh, H. J. Kim, and I. K. Kang, J. Appl. Phys **73**, 6591 (1993).
 [15] J. P. Sethna, K. Dahmen, S. Karta, J. A. Krumhansl, and J. D. Shore, Phys. Rev. Lett. **70**, 3347 (1993)
 [16] K. Dahmen and J. P. Sethna, Phys. Rev. B **53**, 14872 (1996).
 [17] O. Perkovic, K. A. Dahmen, and J. P. Sethna, Phys. Rev. B **59**, 6106 (1999).
 [18] E. Vives and A. Planes, Phys. Rev. B **50**, 3839 (1994).
 [19] E. Vives and A. Planes, Phys. Rev. B **63**, 134431 (2001).
 [20] R. D. Silveira and M. Kardar, Phys. Rev. E **59**, 1355 (1999).
 [21] A. Berger, A. Inomata, J. S. Jiang, J. E. Pearson, and S. D. Bader, Phys. Rev. Lett. **85**, 4176 (2000).
 [22] P. Shukla, Physica A **233**, 235 (1996).
 [23] P. Shukla, Phys. Rev. E **62**, 4725 (2000).
 [24] D. Dhar, P. Shukla, and J. P. Sethna, J. Phys. A **30**, 5259 (1997).
 [25] S. Sabhapandit, P. Shukla, and D. Dhar, J. Stat. Phys. **98**, 103 (2000).
 [26] P. Shukla, Phys. Rev. E **63**, 027102 (2001).
 [27] J. H. Carpenter et al. , J. Appl. Phys. **89**, 6799 (2001).
 [28] G. Bertotti and M. Pasquale, J. Appl. Phys. **67**, 5255 (1990).
 [29] The complete derivation of these equations is quite involved and will thus be reported elsewhere.
 [30] M. Alava, P. Duxbury, C. Moukarzel, and H. Rieger, in *Phase transitions and critical phenomena, Vol 18*, edited by C. Domb and J. Lebowitz (Academic Press, San Diego, 2001).

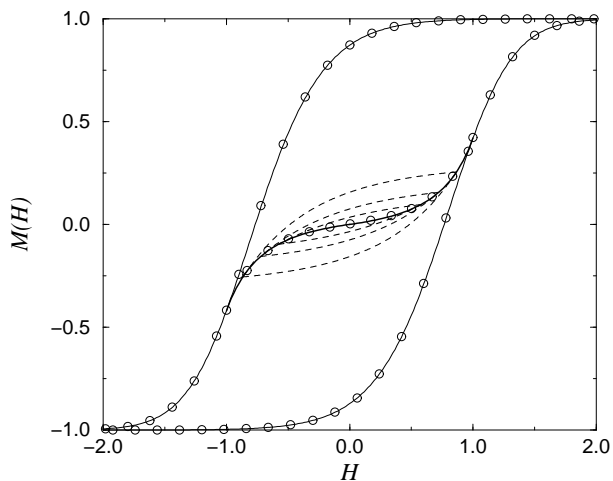


FIG. 1. Exact expressions for the saturation cycle (thin lines), the demagnetization curve (thick lines) and a few minor loops (dotted lines) for $J = 1$ and $R = 1$. The points are the results of a numerical simulation with $L = 5 \cdot 10^5$ spins and a single realization of the disorder.

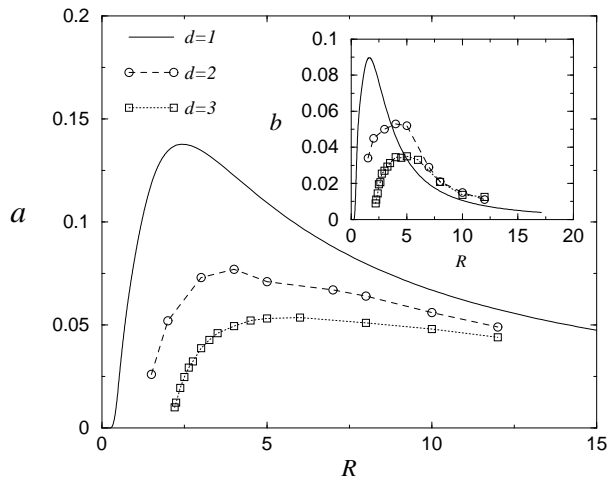


FIG. 2. The reversible susceptibility a computed exactly in $d = 1$ is compared with numerical results in $d = 2$ and $d = 3$. In the inset we show a similar plot for the parameter b .

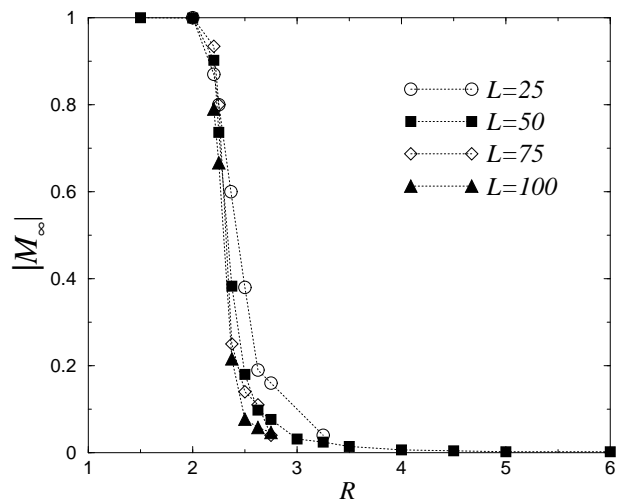


FIG. 3. The absolute value of the final magnetization $|M_\infty|$ as a function of R , obtained from numerical simulations in $d = 3$. For strong disorder $|M_\infty| = 0$ as expected, while for weak disorder the final magnetization coincides with the saturation value. The transition between the two types of behavior becomes sharper as the system size is increased.

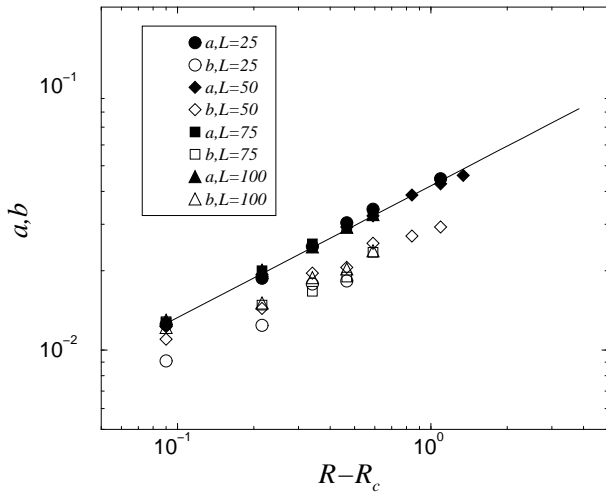


FIG. 4. The Rayleigh parameters a and b scale to zero close to the transition. The results, obtained from numerical simulations in $d = 3$, appear to be quite insensitive to the system size and scale with an exponent roughly equal to $1/2$ (see line).